

Comparison of Ferroelectricity in Isomorphous Lithium Niobate and Lithium Tantalate

M. E. Lines

Bell Telephone Laboratories, Murray Hill, New Jersey 07974

(Received 17 July 1969)

The statistical theory for ferroelectricity developed by the author in an earlier series of papers is used to interpret the dielectric properties of LiNbO_3 and to compare the findings with those obtained in the earlier papers for LiTaO_3 . After evaluating and comparing the microscopic parameters which control the ferroelectric behavior of the two systems, it becomes evident that the major difference between their ferroelectric properties, particularly as regards the Curie temperature, centers around the greater covalency and greater strength of the tantalum-oxygen (compared with the niobium-oxygen) bond. The spontaneous polarization for both salts is found to be 45% ionic, 55% electronic; ionic charges of +1.4 and +0.8 electronic units are calculated for the formal-charge-(+5) ions niobium and tantalum, respectively.

I. INTRODUCTION

In a series of earlier papers,¹ a statistical theory was developed for ferroelectrically ordered systems. The main point of the work was to demonstrate the possibility of describing in a fairly quantitative way the dielectric properties of at least some ferroelectric systems in terms of only a few microscopic parameters; few enough, in particular, for these parameters to be overdetermined by a comparison of theory with experiment.

In terms of the theory, the simplest ferroelectric systems are those which exhibit only a single polar phase, have only a single grossly temperature-dependent-optic-phonon mode (soft mode), and are essentially classical systems (as far as dielectric properties are concerned) over most of the polar phase. The last condition requires that the soft-mode frequency at low temperatures should have an energy $h\nu$, which is less than or of the order kT_C , where T_C is the Curie temperature. The displacement ferroelectrics LiTaO_3 and LiNbO_3 satisfy these conditions fairly well and it was for this reason that one of them, namely, LiTaO_3 , was chosen to test the theory.¹ It was discovered that the dielectric properties of LiTaO_3 were indeed explained in a fairly quantitative manner in terms of the theory and that the theory was self-consistent. The relevant microscopic parameters were determined and their accuracy roughly estimated.

In the present paper, the calculations are repeated for isomorphous LiNbO_3 and a comparison made between the tantalate and niobate salts. Such a comparison is particularly interesting for this case because, in spite of their isomorphous structures in both the polar and nonpolar phases,

some of their dielectric properties [and particularly their Curie temperatures² 890 °K (LiTaO_3) and 1470 °K (LiNbO_3)] are surprisingly different.

After evaluating and comparing the microscopic parameters which determine the ferroelectric behavior of the two systems, it becomes evident that a major difference between these ferroelectrics centers around the greater strength of the tantalum-oxygen bond (compared with niobium-oxygen). The effect reduces the Curie temperature of the tantalate, with respect to the niobate, by increasing the stiffness of the local contribution to the soft mode and thus making it more difficult for the negative contribution from the dipolar forces to bring about the transition to the double minimum potential and the onset of ferroelectricity.

The Curie-temperature difference is made even more dramatic by the greater degree of covalency found for the tantalate, which decreases the effective point charges and hence, decreases the dipolar forces in LiTaO_3 with respect to LiNbO_3 .

In Sec. II, we present the effective Hamiltonian in whose terms the statistical theory is cast, and evaluate the microscopic parameters it contains for the case of LiNbO_3 by a direct comparison of theory with experiment. These parameters are then compared with those determined earlier¹ for LiTaO_3 . In Sec. III, the results are analyzed in the light of the findings³ that intercell correlation effects for ionic motion must be recognized. We find that for LiNbO_3 , just as for LiTaO_3 , the ionic motion is very dominantly correlated to temperatures of the order of (and almost certainly above) the very elevated Curie temperature. Finally, effective ionic charges, electronic polarizabilities, bonding frequencies, etc., are calculated and compared for the two salts.

II. ANALYSIS OF EXPERIMENTAL DATA FOR LiNbO₃

Following the development of the statistical theory as given in Ref. 1, we describe the dielectric properties of LiNbO₃ in terms of an effective Hamiltonian

$$v\mathcal{H}_{\text{eff}} = \frac{1}{2}(\pi^2 + \omega_0^2 \xi^2) + A\xi^4 + B\xi^6 - \eta S\xi(E + \gamma \langle P_{\text{ion}} \rangle) , \quad (2.1)$$

where π and ξ are, respectively, the conjugate-momentum and displacement coordinates of the soft mode of lattice vibration, v is the volume of a primitive cell of the crystal lattice, E is the applied (Maxwell) field taken to be in the direction of the polar axis, and

$$P_{\text{ion}} = (S/v)\xi , \quad (2.2)$$

where S is an effective-charge parameter. The microscopic interpretation of the parameters ω_0, A, B, η, S , and γ involved has been given in the preceding paper³ and will be set out further in Sec. III. The angular brackets in Eq. (2.1) represent an ensemble (thermal) average, $\langle P_{\text{ion}} \rangle$ being the thermodynamic ionic polarization. Since v is directly measurable from x-ray or neutron diffraction studies, Eq. (2.1) contains five parameters to be determined by comparing the results of a statistical calculation with experiment, viz., $\omega_0, A, B, \eta S$, and γS . The total polarization $\langle P \rangle$ we relate to its ionic part $\langle P_{\text{ion}} \rangle$ by

$$\langle P \rangle = \eta' \langle P_{\text{ion}} \rangle = (\eta' S/v) \langle \xi \rangle \quad (2.3)$$

in the absence of applied field, defining a sixth "unknown" $\eta' S$. We take η' to be frequency independent, thereby restricting ourselves to a range of frequencies well below the onset of electronic transitions. The six microscopic parameters determining the general dielectric behavior of LiNbO₃ may now be determined by a comparison of theory with experiment.

A. Dielectric Constant

At temperatures approaching the transition temperature T_C , the contribution of the soft mode to dielectric constant becomes very large and the one soft-mode approximation is at its best. Experimentally, susceptibility data are only available up to about 1200 °K ($\approx 0.82 T_C$) and follow a Curie-Weiss law over a wide temperature range.⁴ However, the Curie-Weiss intercept is some 120 °K below T_C and indicates (not, as suggested in Ref. 4, the possibility of a first-order phase change, which would require an intercept above T_C) that the relationship is spurious in the sense that the parameters which it defines are not related to those in the theoretically derived Curie-Weiss law for the $T \rightarrow T_C$ limit. To make use of theory,

it is necessary to extrapolate the susceptibility to infinity at T_C by allowing for a deviation from Curie-Weiss behavior in this region. This we have done by appealing to the experimental results for LiTaO₃⁵ which are available right up to T_C . These measurements for isomorphous LiTaO₃, when plotted as a function of $T_C - T$, join very smoothly onto the LiNbO₃ data (see Fig. 1) and are therefore very probably indicative of the behavior of the susceptibility of LiNbO₃ in the critical region. With this assumption we find, as $T \rightarrow T_C$, the relationship

$$\epsilon_{\text{ferro}} = (0.75 \times 10^5) / (T_C - T) . \quad (2.4)$$

Theoretically, the corresponding result is¹

$$\epsilon_{\text{ferro}} = (4\pi\eta'/\gamma)[T_C/(T - T_C)]\Phi_f^{-1} , \quad (2.5)$$

where $\Phi_f = 2\mu' - \frac{4}{3}$, and where μ' as a function of the relevant microscopic parameters has been computed in part I of Ref. 1. We deduce

$$\eta'/\gamma = 8.1 \left(\frac{2}{3} - \mu' \right) . \quad (2.6)$$

At low temperatures, the contribution of the soft mode to the dielectric constant (sometimes called the strength of the mode) has been measured by Barker and Loudon⁶ to be $s = 16.0$ from a study of the infrared reflection spectra. Theoretically, it is given by¹

$$s = 4\pi\eta'S^2/[v\omega^2(T)] , \quad (2.7)$$

where $\omega(T)$ is the soft-mode frequency at temperature T .

It is useful to analyze many of the data in terms of a convenient pair of dimensionless parameters defined as follows¹:

$$\alpha'/\beta' = (\eta\gamma S^2/v)/\omega_0^2, \quad (\beta')^{1/2}/\delta = -A/(B\eta\gamma S^2/v) . \quad (2.8)$$

This pair of temperature-independent parameters determines the nature of the phase transition, i. e., first- or second-order, displacement or order-disorder ferroelectric, etc., as shown in Fig. 2. The former measures the ratio of effective-field energy to the harmonic-contribution energy, and the latter is, in a sense, a measure of quartic anharmonicity. As in LiTaO₃, we shall find ourselves concerned with the case of negative quartic anharmonicity.

B. Soft-Mode Frequency

The temperature dependence of the soft-mode frequency in the ferroelectric phase of LiNbO₃ has been measured both by a study of infrared reflection spectra⁶ and of Raman spectra.^{6, 7} At very low temperatures, the soft-mode frequency approaches 258 cm⁻¹. At room temperature the frequency has decreased slightly to 248 cm⁻¹

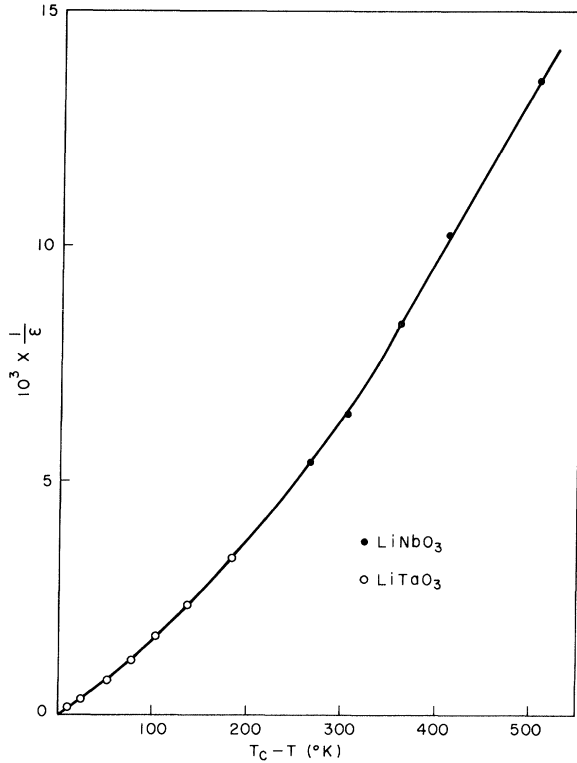


FIG. 1. Plot of reciprocal susceptibility versus $(T_C - T)$, where T_C is the Curie temperature for LiNbO_3 and LiTaO_3 taken from the experimental measurements reported in Refs. 4 and 5, respectively, and showing the smooth join of the published data at $T_C - T \sim 250^\circ\text{K}$.

and at higher temperatures (in fact, from room temperature right up to the Curie point) it follows fairly closely the law

$$\omega(T) = 280[(T_C - T)/T_C]^{1/2} \text{ cm}^{-1}.$$

Coupling Eq. (2.7) with the definition in (2.8) of α'/β' , and giving the mode strength the value 16 as measured by Barker and Loudon,⁶ we find that

$$\omega^2(300)/\omega_0^2 = \frac{4}{16} \pi(\alpha'/\beta')(\eta'/\gamma). \quad (2.9)$$

Noting that $\omega(300)/\omega(0) = \frac{248}{258}$ and using Eq. (2.6), this reduces to

$$\omega^2(0)/\omega_0^2 = 6.9(\alpha'/\beta')(\frac{2}{3} - \mu'). \quad (2.10)$$

Now, $\omega^2(0)/\omega_0^2$ and μ' have been calculated quite generally as functions of β'/α' and $\beta'^{1/2}/\delta$ in parts I and II of Ref. 1. Thus, Eq. (2.10) defines a relationship between these dimensionless parameters; we have sketched it in Fig. 3 [curve (i)].

For higher temperatures, both theory and experiment suggest the law $\omega(T) \propto (T_C - T)^{1/2}$. Consider first a small anharmonicity approximation valid for $\beta'/\alpha' \rightarrow 1$, $(\beta')^{1/2}/\delta \rightarrow 0$. In this limit,

theory¹ predicts

$$\omega^2(T)/\omega_0^2 = 2(\frac{2}{3} - \mu')(T_C - T)/T_C. \quad (2.11)$$

Experimentally, this form holds right down to room temperature. If this is to hold theoretically also, we must have

$$\omega^2(300)/\omega_0^2 = 1.59(\frac{2}{3} - \mu'). \quad (2.12)$$

Using Eqs. (2.9) and (2.6), this reduces directly to $\beta'/\alpha' = 4.0$. This tells us immediately that the small anharmonicity approximation is not appropriate for LiNbO_3 . The extension of the above procedure to larger values of anharmonicity has been discussed in Ref. 1 and requires numerical computations of some complexity. We need not repeat the details here except to quote the result, viz., $\beta'/\alpha' = 2.0 \pm 0.5$, where the error brackets result from approximate numerical integrations coupled with other approximations detailed in parts II and III of Ref. 1.

Coupling these data with the restrictions on β'/α' and $\beta'^{1/2}/\delta$, resulting from the knowledge that LiNbO_3 is a displacement ferroelectric^{6, 8, 9} (microscopically centrosymmetric nonpolar phase), and has a second-order or nearly second-order phase transition^{10, 11} and a soft-mode frequency⁷ going to (or very close to) zero at T_C , can be seen

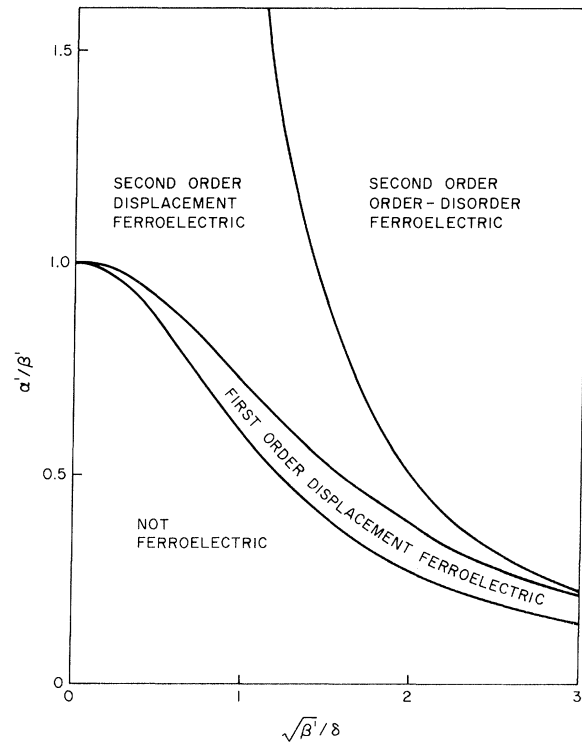


FIG. 2. Diagram indicating the manner in which the parameters α'/β' and $\beta'^{1/2}/\delta$, defined in the text, determine the nature of the ferroelectric phase transition.

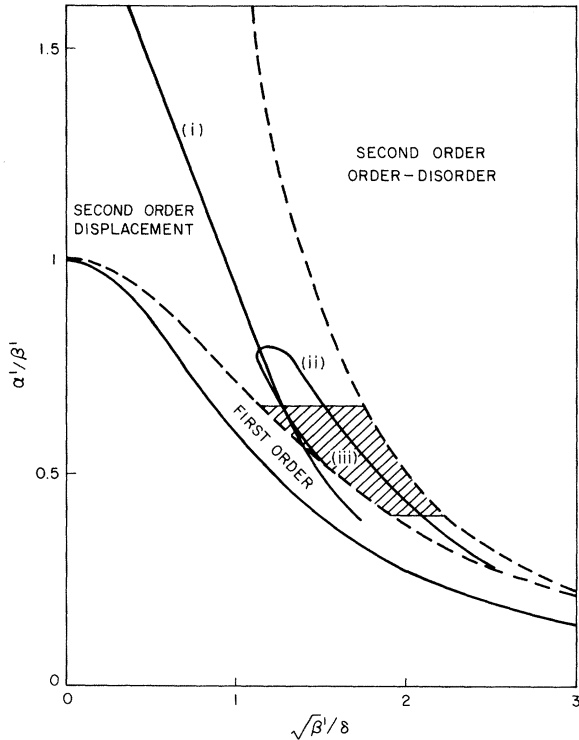


FIG. 3. A number of curves each derived from the experimental data for LiNbO_3 compared on a α'/β' , $\beta'^{1/2}/\delta$ plot. Curve (i) is derived from the soft-mode frequency at low temperatures, curve (ii) from the value of spontaneous polarization at low temperatures, and the shaded area (iii) contains points consistent with the findings for soft-mode frequency near the Curie temperature combined with the limits (dashed curves) that the transition is of a displacement type and of second order. The shape of the polarization curve versus temperature suggests that the transition is very close to being first order, restricting the allowed α'/β' , $(\beta')^{1/2}/\delta$ values to points near to the lower dashed curve.

from Fig. 2 to confine the possible values of these dimensionless parameters for LiNbO_3 to quite a small region; the latter is shown shaded in Fig. 3.

C. Crystal Structure Data

Single-crystal x-ray and neutron-diffraction studies on LiNbO_3 have been carried out by Abrahams *et al.*^{9, 12, 13} Below the Curie temperature the crystal space group is $R3c$ and above the Curie temperature it is very probably $R\bar{3}c$, which is centrosymmetric. The structure is isomorphic with LiTaO_3 , which has been discussed and sketched in Ref. 1. In going to the ferroelectric phase, the ions move with respect to their center of mass and, at room temperature, the magnitudes of the respective shifts along the polar axis are $q(\text{Li}) = 0.51 \text{ \AA}$, $q(\text{O}) = -0.20 \text{ \AA}$, and $q(\text{Nb}) = 0.062 \text{ \AA}$.

The variable ξ of Hamiltonian (2.1) is defined in terms of the q 's in the one soft-mode approximation by¹

$$q_b = u_b \xi, \quad \sum_b M_b u_b^2 = 1, \quad (2.13)$$

where the sum runs over all ions in a primitive cell, and where M signifies mass. Using Eqs. (2.13) in conjunction with the measured shifts for LiNbO_3 , we find that $\langle \xi \rangle = 2.86 \text{ amu}^{1/2} \text{ \AA}$ at room temperature. This is of great interest since the spontaneous polarization is expressible in terms of $\langle \xi \rangle$ via the equation

$$\langle P \rangle = \eta' (S/v) \langle \xi \rangle. \quad (2.14)$$

Putting the soft-mode strength at room temperature equal to 16.0 and using Eq. (2.7) we find that

$$\langle P \rangle^2 = [4\eta' \omega^2(300)/\pi v \eta] \langle \xi \rangle^2. \quad (2.15)$$

Everything in this equation is known except the ratio η/η' . Putting the room-temperature value of spontaneous polarization equal to¹⁴ $71 \pm 2 \mu\text{C}/\text{cm}^2$, the primitive cell volume v (two formula weights) = $106 \times 10^{-24} \text{ cm}^3$, and $\omega(300) = 248 \text{ cm}^{-1}$, we calculate $\eta/\eta' = 0.79$.

D. Spontaneous Polarization as $T \rightarrow 0$

In part I of Ref. 1, a rather simple relationship was deduced between the low-temperature spontaneous polarization $\langle P_0 \rangle$ and the Curie temperature T_C . We may write it

$$kT_C = \rho' v (\gamma/\eta') (\eta/\eta') \langle P_0 \rangle^2, \quad (2.16)$$

where ρ' as a function of β'/α' and $(\beta')^{1/2}/\delta$ has been computed in part I of Ref. 1. This equation as it stands implies no simple relationship between Curie temperature and saturation polarization over a range of ferroelectrics, since nothing is presently known about the variation of η , η' , γ , etc., from system to system. Nevertheless, it is very interesting to note that just such a simple relationship has been found experimentally¹⁵ to hold with a fair degree of accuracy over quite a range of displacement ferroelectrics. The observation suggests that $T_C \propto \langle P_0 \rangle^2$ and therefore, that $\rho' v (\gamma/\eta') (\eta/\eta')$ does not vary much over this group of ferroelectrics.

Substituting the experimental values for Curie temperature ($1470 \text{ }^\circ\text{K}$) and $\langle P_0 \rangle$ ($72 \mu\text{C}/\text{cm}^2$) and using the value $\eta/\eta' = 0.79$ already determined, we reduce Eq. (2.16) to a relationship between ρ' (i.e., the dimensionless parameters β'/α' and $\beta'^{1/2}/\delta$), and η'/γ . Now, eliminating η'/γ between Eqs. (2.16) and (2.6) provides another relationship between the dimensionless parameters which we show as curve (ii) of Fig. 3.

E. Spontaneous Polarization as a Function of Temperature

The first suggestion that the polarization curve

of LiNbO₃ might be much more steplike than it is in LiTaO₃ came from the measurement of the nonlinear d_{33} coefficient from second harmonic generation experiments.¹¹ A close relationship between d_{33} and polarization had already been observed in BaTiO₃¹⁶ and some theoretical insight into the relationship obtained.¹⁷ This finding was confirmed by Glass¹⁰ who measured the pyroelectric coefficient for LiNbO₃, using the dynamic technique first used by Chynoweth.¹⁸ By degree of steplike character, in the present context, we are not referring to a discontinuity but to a measure of the radius vector of a P/P_0 -versus- T/T_C plot when $P/P_0 = T/T_C$. For lithium tantalate this value is 1.04; for lithium niobate it is of order 1.15–1.20. For a step-function polarization limit, this quantity would, of course, be $\sqrt{2}$. From the theory of Ref. 1 as computed in part I of that set of papers, no curves with steplike character greater than 1.10 were found and the more steplike of these were for order-disorder ferroelectrics. Moreover, for the possible range of β'/α' and $\beta'^{1/2}/\delta$ parameters allowed by the curves in Fig. 3 for LiNbO₃, the theoretical polarization curve shapes have steplike character of only about 1.00.

Any of three explanations of this apparent disagreement between theory and experiment seems possible. First, the negative anharmonicity contributions to lattice potential energy may be of higher degree than fourth in LiNbO₃. This would increase the steplike character of the associated polarization curves. Indeed, the magnitude of the ferroelectric distortion in LiNbO₃ may be large enough to make any truncated series expansion in terms of mode parameter of questionable quantitative value for this case. Second, it is possible that the phase transition is just first order (see Fig. 3) and that the lack of an observable sharp transition is due to crystal inhomogeneity or lack of stoichiometry. Finally, it is possible that LiNbO₃ is a second-order ferroelectric but has dielectric parameters which put it very close indeed to the first-second-order boundary. That this is quite possible from the data examined to date is seen from Figs. 2 and 3. The variation of polarization curve shape in the immediate vicinity of the first-second-order boundary has not yet been computed for the general case; indeed, the boundary itself has not yet been located with precision outside the small anharmonicity realm.¹ The problem is solely a computational one involving the simultaneous solution of integral equations. However, for small anharmonicities the integrations involved can be performed analytically and the equations correspondingly simplify very considerably. For small anharmonicities¹⁹ it is

found that polarization curve shapes become very sensitive to β'/α' and $\beta'^{1/2}/\delta$ when the latter are very close to the second-first-order boundary, their steplike character increasing by $\sim 10\%$ as the boundary is approached. The more pertinent calculations outside the small anharmonicity region have not yet been carried out but, if a similar phenomenon persists for larger anharmonicities, it may be possible to explain the steplike character of the LiNbO₃ curves within the framework of the theory of Ref. 1, while retaining a second-order transition.

The final piece of experimental evidence used in conjunction with the assessment of the theory for LiTaO₃ was the specific-heat anomaly at the Curie temperature. For LiNbO₃ the anomaly has been observed,²⁰ but the reported accuracy of the measurements is insufficient to attach much quantitative significance to the results.

We are now in a position to estimate the effective Hamiltonian parameters for LiNbO₃. From Fig. 3, coupled with our above result that the LiNbO₃ system is probably very close to the second-first-order boundary, we estimate values

$$\beta'/\alpha' = 1.9 \pm 0.5, \quad (\beta')^{1/2}/\delta = 1.5 \pm 0.4. \quad (2.17)$$

Using the median values, it follows that $1^{\frac{2}{3}} - \mu' \approx 0.77$ and $\beta'_C \approx 0.37$, where the latter parameter controls the Curie temperature through the equation¹

$$kT_C = (1/B)^{1/2} (\eta\gamma S^2/v)^{3/2} (\beta'_C)^{3/2}. \quad (2.18)$$

Thus, from Eq. (2.6), we find that $\eta'/\gamma \sim 6$. Equation (2.14) coupled with the room-temperature measured values for polarization and distortion from centrosymmetry, yields directly $\eta'S \approx 620 \text{ cm}^3/2 \text{ sec}^{-1}$ and from this we can calculate

$$(\eta\gamma S^2/v)^{1/2} = (\eta'S)(\eta/\eta')^{1/2} (\gamma/\eta')^{1/2} \\ \times (1/v)^{1/2} \approx 114 \text{ cm}^{-1}. \quad (2.19)$$

This, in turn, leads to

$$\omega_0 = (\beta'/\alpha')^{1/2} (\eta\gamma S^2/v)^{1/2} \approx 157 \text{ cm}^{-1}. \quad (2.20)$$

Finally, we estimate

$$-A/B^{1/2} = (\sqrt{\beta'}/\delta)(\eta\gamma S^2/v)^{1/2} \approx 171 \text{ cm}^{-1}, \quad (2.21)$$

and, from Eq. (2.18) with $T_C = 1470 \text{ }^\circ\text{K}$, the value $B \sim 4k \text{ amu}^{-3} \text{ \AA}^{-6}$ leading to $A \sim -70k \text{ amu}^{-2} \text{ \AA}^{-4}$.

This completes the determination of the effective Hamiltonian parameters and we list them in Table I, where we also include, for comparison, the equivalent findings for LiTaO₃ taken from Ref. 1. Also included in Table I are rough estimates for the accuracy of the findings. These error brackets include assessments of experimental accuracy but are dominated for both salts by the spread in

TABLE I. Effective Hamiltonian parameters for lithium tantalate and lithium niobate.

LiTaO ₃	LiNbO ₃
$v = 106 \times 10^{-24} \text{ cm}^3$	$v = 106 \times 10^{-24} \text{ cm}^3$
$\omega_0 = 140 \text{ cm}^{-1} (\pm 20\%)$	$\omega_0 = 157 \text{ cm}^{-1} (\pm 25\%)$
$-A/\sqrt{B} = 176 \text{ cm}^{-1} (\pm 25\%)$	$-A/\sqrt{B} = 171 \text{ cm}^{-1} (\pm 25\%)$
$A = -90 \text{ k amu}^{-2} \text{ \AA}^{-4}$ ($\pm 300\%$)	$A = -70 \text{ k amu}^{-2} \text{ \AA}^{-4}$ ($\pm 300\%$)
$B = 6 \text{ k amu}^{-3} \text{ \AA}^{-6}$ ($\pm 300\%$)	$B = 4 \text{ k amu}^{-3} \text{ \AA}^{-6}$ ($\pm 300\%$)
$\eta'S = 520 \text{ cm}^{3/2} \text{ sec}^{-1}$ ($\pm 10\%$)	$\eta'S = 620 \text{ cm}^{3/2} \text{ sec}^{-1}$ ($\pm 10\%$)
$\eta/\eta' = 1.3 (\pm 10\%)$	$\eta/\eta' = 0.8 (\pm 10\%)$
$\eta'/\gamma = 13 (\pm 10\%)$	$\eta'/\gamma = 6 (\pm \frac{15}{40}\%)$

values of β'/α' and $(\beta')^{1/2}/\delta$, which ensures the self-consistency of the method. The reason why the substantially increased error bracket for η'/γ in LiNbO₃ (compared with LiTaO₃) is not reflected in increased uncertainties for the other parameters rests with our belief that LiNbO₃ is very close to being a first-order ferroelectric, thereby correlating η'/γ with β'/α' and $\beta'^{1/2}/\delta$ within the error brackets expressed in Eq. (2.17). That is, in addition to Eq. (2.17), we have restricted the latter parameters to values close to the first-second-order boundary (Fig. 3).

From Table I we can now compare the relevant microscopic parameter values for the two salts. Using the microscopic model (point-charges plus electronic polarizabilities) outlined in the preceding paper³ to represent LiNbO₃ and LiTaO₃ in turn, we can now interpret the Table I parameter similarities and differences for the salts in terms of familiar microscopic concepts.

III. LiTaO₃ AND LiNbO₃: AN ANALYSIS OF THE RESULTS

The Hamiltonian parameters of Table I can be directly related to effective charges e_b and ionic displacements $q_b = u_b \xi$, where $\sum_b M_b u_b^2 = 1$, and where M_b is the mass of the b th ion and the summation runs over all sites b in a primitive cell. The relevant equations are³

$$S = \sum_b e_b u_b, \quad (3.1)$$

$$\eta S = \sum_b (1 + \eta'_{\text{RPA}} \gamma_{\text{RPA}}^b \alpha) e_b u_b, \quad (3.2)$$

$$\eta \gamma S = \sum_b \eta'_{\text{RPA}} \gamma^b e_b u_b, \quad (3.3)$$

$$\text{where } \alpha = (1/v) \sum_b \alpha_b, \quad (3.4)$$

α_b is the electronic polarizability of the b th ion, and where

$$\eta'_{\text{RPA}} \equiv \eta' = [1 - (1/v) \sum_b \alpha_b \gamma_{\text{RPA}}^b]^{-1}, \quad (3.5)$$

in which γ_{RPA}^b are the "effective-field" Lorentz

parameters³ at sites b .

In the preceding paper,³ we show how an interpretation of the Hamiltonian parameters assuming a complete randomness approximation for neighbor cell ionic motions [which amounts to putting γ^b of Eq. (3.3) equal to γ_{RPA}^b of Eq. (3.2)] leads to a number of inconsistencies for LiTaO₃. An exactly equivalent situation holds for the LiNbO₃ data and we assume an approximation in which possible correlations are allowed for intercell ionic motions. Following Ref. 3, we separate the Lorentz field contributions into a correlated part $\gamma_{\text{corr}}^b P_{E=0}$ and a completely uncorrelated part $\gamma^b \langle P \rangle_{E=0}$ in such a way that

$$\gamma_{\text{RPA}}^b = \gamma^b + \gamma_{\text{corr}}^b \quad (3.6)$$

for all b . With such a definition we find that³

$$\omega_0^2 = \Omega_0^2 - (\eta \gamma_{\text{corr}} S^2 / v), \quad (3.7)$$

$$\text{where } \eta \gamma_{\text{corr}} S = \sum_b \eta'_{\text{RPA}} \gamma_{\text{corr}}^b e_b u_b, \quad (3.8)$$

and where Ω_0 describes the frequency of the soft mode in the complete absence of dipolar forces, i. e., the bonding frequency of the soft mode.

For LiNbO₃, we first estimate η'_{RPA} from the measured high-frequency dielectric constant⁶

$$\epsilon_\infty(\text{LiNbO}_3) = 4.6 = 1 + 4\pi \eta'_{\text{RPA}} \alpha$$

using the simplified equation

$$\eta'_{\text{RPA}} = (1 - \frac{4}{3} \pi \alpha)^{-1}, \quad (3.9)$$

which is rigorous only for certain cubic structures, but which was found to be quite quantitative for LiTaO₃ and gives a consistent value for the polarizability of the niobate ion $\alpha(\text{NbO}_3)$ over a range of different structures. We find, from the above LiNbO₃ data, a niobate polarizability $\alpha(\text{NbO}_3) = 6.9 \text{ \AA}^3$ and values $\eta'_{\text{RPA}} = 2.20$ and $\alpha = 0.130$, where

$$\alpha = (1/v) [2\alpha(\text{Li}) + 2\alpha(\text{NbO}_3)], \quad (3.10)$$

in which $\alpha(\text{NbO}_3) = \alpha(\text{Nb}) + 3\alpha(\text{O})$,

and where the factors two arise from the fact that the primitive cell contains two formula weights (2 fw) for LiNbO₃. The electronic polarizability of lithium is negligibly small in the present context $\alpha(\text{Li}) \approx 0.03$.²¹ In the same manner, a niobate polarizability can be calculated for Ba₂NaNb₅O₁₅ [for which^{22, 23} $\epsilon_\infty = 4.6$ and $v(4 \text{ fw}) = 1240 \text{ \AA}^3$] and for Ba_{21.25}Sr_{3.75}Nb₁₀O₃₀ [for which^{24, 25} $\epsilon_\infty = 4.9$ and $v(1 \text{ fw}) = 605 \text{ \AA}^3$]. Making use of generally accepted values $\alpha(\text{Ba}) \approx 2.5$, $\alpha(\text{Sr}) \approx 1.6$, and $\alpha(\text{Na}) \approx 0.4$ in units of \AA^3 , as taken from Tessman, Kahn, and Shockley,²¹ we find that $\alpha(\text{NbO}_3) = 7.0 \text{ \AA}^3$ in Ba₂NaNb₅O₁₅ and $\alpha(\text{NbO}_3) = 7.2 \text{ \AA}^3$ in the barium strontium salt. The consistency of the findings lends some support to the concept of

a well-defined niobate electronic polarizability. We neglect any possible small temperature dependence of polarizability.

Using the above finding $\eta'_{\text{RPA}} = 2.20$ for LiNbO_3 , we may relate the ionic polarization at low temperatures (i. e., spontaneous polarization divided by η'_{RPA}) to effective ionic charges $e(\text{Li})$, $e(\text{Nb})$, and $e(\text{O})$ through the equation

$$\sum_b e_b q_b = \langle P \rangle / \eta'_{\text{RPA}} \quad , \quad (3.11)$$

where^{9, 26} $q(\text{Li}) = 0.51 \text{ \AA}$, $q(\text{Nb}) = 0.062 \text{ \AA}$, and $q(\text{O}) = -0.20 \text{ \AA}$ are the room-temperature spontaneous ionic displacements from centrosymmetry and $\langle P \rangle$ at room temperature is¹⁴ 71 C/cm^2 . We find that

$$0.51 e(\text{Li}) + 0.062 e(\text{Nb}) - 0.60 e(\text{O}) = 1.07 \quad , \quad (3.12)$$

where e is measured in electronic units. Allowing for charge conservation,

$$e(\text{Li}) + e(\text{Nb}) + 3e(\text{O}) = 0 \quad , \quad (3.13)$$

and taking $e(\text{Li})$ to be +1, we calculate effective charges $e(\text{Nb}) = +1.4$ and $e(\text{O}) = -0.8$.

An equivalent calculation for LiTaO_3 yields³ $\alpha(\text{TaO}_3) = 6.8 \text{ \AA}^3$, $\eta'_{\text{RPA}} = 2.17$, $e(\text{Ta}) = 0.8$, and $e(\text{O}) = -0.6$. Thus, the niobate and tantalate ion groups have closely similar electronic polarizabilities, but the degree of covalency of the latter is markedly larger. The larger covalency of the tantalate is in broad agreement with effective-mass data in tantalates and niobates, i. e., the greater the principal quantum number, the greater the overlap with the oxygen ions resulting in broader conduction band widths. The result also agrees with that expected from electronegativity differences, and the actual effective charge numbers are in close agreement with those determined from nuclear quadrupole resonance experiments.²⁷

From the LiNbO_3 data of Table I we find, putting $\eta' = \eta'_{\text{RPA}} = 2.20$, that

$$\eta \approx 1.8, \quad \gamma \approx 0.37, \quad S \approx 282 \text{ cm}^{3/2} \text{ sec}^{-1} \quad . \quad (3.14)$$

Also, from Eqs. (3.2) and (3.3) it follows, for LiNbO_3 ,

$$\sum_b \gamma_{\text{RPA}}^b e_b u_b \sim 2.8S \quad , \quad (3.15)$$

$$\sum_b \gamma^b e_b u_b \sim 0.30S \quad , \quad (3.16)$$

and, from Eqs. (3.6) and (3.8),

$$\sum_b \gamma_{\text{corr}}^b e_b u_b \sim 2.5S \quad . \quad (3.17)$$

Finally, from Eq. (3.7), we calculate a bonding frequency $\Omega_0 = 377 \text{ cm}^{-1}$. These results are summarized in Table II together with the equivalent findings for LiTaO_3 and a rough estimate of the accuracy of the results.

In comparing the results for LiTaO_3 and LiNbO_3 ,

it is evident that the electronic properties are much more alike than the ionic ones. The polarizabilities of the tantalate and niobate ionic groups are equal to within the accuracy of the data, and the equality of the η'_{RPA} parameters indicate that electronic and ionic contributions to spontaneous polarization make up the same proportions (55% and 45%, respectively) for both salts. There are, however, some significant differences between some of the other parameters in Table II. The difference in the η parameters of Eq. (3.2) follows directly from the measured difference in the soft-mode strengths at room temperature [see Eq. (2.7)] which are 16 and 30 for LiNbO_3 and LiTaO_3 , respectively.^{6, 28} It signifies, most probably, that the ionic motion in the soft modes of both salts is not strictly along the polar axis (although, by symmetry,⁶ the resultant total mass movement of the entire mode is so restricted) but, rather, that compensating lateral components of oxygen ionic motion exist,⁶ and to a significantly different degree for the two systems. Finally, the much larger ratio

$$\frac{\sum_b \gamma^b e_b u_b}{\sum_b \gamma_{\text{RPA}}^b e_b u_b}$$

for the niobate than the tantalate (0.11 compared to 0.03) is an indication of a markedly smaller degree of ionic correlation (as defined in Ref. 3) in LiNbO_3 than in LiTaO_3 near their respective Curie temperatures. This effect probably reflects no more than the fact that ionic correlation effects are a decreasing function of temperature and that T_C (LiNbO_3) is some several hundred degrees higher than T_C (LiTaO_3). However, the smallness of the numerical value of the above ratio, even for the niobate, is an indication that correlation effects are still enormously important – even at $1500 \text{ }^\circ\text{K}$.

As for the difference in Curie temperature itself ($890 \text{ }^\circ\text{K}$ for LiTaO_3 and $1470 \text{ }^\circ\text{K}$ for LiNbO_3), there are probably many factors involved in a detailed explanation, e. g., anharmonicity, bonding forces, Lorentz parameters, and covalency effects. Our first observation, however, is that the difference is not surprisingly large in spite, perhaps, of initial reactions to the contrary. The covalency contribution alone, which affects T_C (through the effective charge strengths) as S^2 , could account for $\frac{2}{3}$ of the observed difference. Of the other effects, the difference in bonding frequencies also favors a higher niobate Curie temperature, but this effect may be somewhat reduced by the smaller Lorentz mode parameter in LiNbO_3 . Our accuracy is not sufficient to allow us to decide whether anharmonicity differences also contribute. In summary, it is probably fair to say that the higher niobate T_C is primarily due

TABLE II. Comparison of microscopic dielectric parameters for lithium tantalate and lithium niobate, and a semiquantitative assessment of the accuracy of the findings.

Property	LiTaO_3	LiNbO_3
Electronic polarizability α	0.127 ($\pm 2\%$)	0.130 ($\pm 2\%$)
$\eta_{\text{RPA}}^r = \langle P \rangle / \langle P_{\text{ion}} \rangle$	2.17 ($\pm 2\%$)	2.20 ($\pm 2\%$)
Effective ionic charge parameter S	240 $\text{cm}^{3/2} \text{sec}^{-1}$ ($\pm 15\%$)	282 $\text{cm}^{3/2} \text{sec}^{-1}$ ($\pm 15\%$)
Effective Ta(Nb) ionic charge	0.8 ($\pm 25\%$)	1.4 ($\pm 25\%$)
Effective oxygen ionic charge	-0.6 ($\pm 15\%$)	-0.8 ($\pm 15\%$)
Hamiltonian parameter γ	0.17 ($\pm 15\%$)	0.37 ($\pm 40\%$)
Hamiltonian parameter η	2.8 ($\pm 15\%$)	1.8 ($\pm 15\%$)
$\frac{\sum_b \gamma_{\text{RPA}}^b e_b u_b}{\sum_b \gamma^b e_b u_b}$	6.5 ($\pm 20\%$)	2.8 ($\pm 30\%$)
$\frac{\sum_b \gamma^b e_b u_b}{\sum_b e_b u_b}$	0.22 ($\pm 20\%$)	0.30 ($\pm 50\%$)
Bonding frequency Ω_0	479 cm^{-1} ($\pm 10\%$)	377 cm^{-1} ($\pm 15\%$)

to two factors: the larger effective charges (smaller degree of covalency of the niobate ion group), and the smaller bonding frequency (weaker short-range forces) of LiNbO_3 with respect to LiTaO_3 .

ACKNOWLEDGMENTS

The author is pleased to acknowledge informative discussions with S. C. Abrahams and A. M. Glass. Comments on the final manuscript by M. DiDomenico were also greatly appreciated.

¹M. E. Lines, Phys. Rev. **177**, 797 (1969); **177**, 812 (1969); **177**, 819 (1969).

²A. A. Ballman, H. J. Levinstein, C. D. Capio, and H. Brown, J. Am. Ceram. Soc. **12**, 657 (1967); J. G. Bergman, A. Ashkin, A. A. Ballman, J. M. Dziedzic, H. J. Levinstein, and R. G. Smith, Appl. Phys. Letters **12**, 92 (1968).

³M. E. Lines, preceding paper, Phys. Rev. B **2**, 690 (1970).

⁴K. Nassau, H. J. Levinstein, and G. M. Loiacono, J. Phys. Chem. Solids **27**, 989 (1966).

⁵A. M. Glass, Phys. Rev. **172**, 564 (1968).

⁶A. S. Barker, Jr., and R. Loudon, Phys. Rev. **158**, 433 (1967).

⁷I. P. Kaminow and W. D. Johnston, Jr., Phys. Rev. **168**, 1045 (1968).

⁸R. C. Miller and A. Savage, Appl. Phys. Letters **9**, 169 (1966).

⁹S. C. Abrahams, J. M. Reddy, and J. L. Bernstein, J. Phys. Chem. Solids **27**, 1019 (1966).

¹⁰A. M. Glass (unpublished).

¹¹R. C. Miller, Phys. Rev. **134**, A1313 (1966).

¹²S. C. Abrahams, J. M. Reddy, and J. L. Bernstein, J. Phys. Chem. Solids **27**, 997 (1966).

¹³S. C. Abrahams, W. C. Hamilton, and J. M. Reddy, J. Phys. Chem. Solids **27**, 1013 (1966).

¹⁴S. H. Wemple, M. DiDomenico, and I. Camlibel,

Appl. Phys. Letters **12**, 209 (1968).

¹⁵S. C. Abrahams, S. K. Kurtz, and P. B. Jamieson, Phys. Rev. **172**, 551 (1968).

¹⁶R. C. Miller (private communication reported in Ref. 5).

¹⁷S. K. Kurtz and F. N. H. Robinson, Appl. Phys. Letters **10**, 63 (1967).

¹⁸A. G. Chynoweth, J. Appl. Phys. **27**, 78 (1956).

¹⁹M. E. Lines (unpublished).

²⁰L. B. Pankratz and E. G. King, U.S. Department of the Interior, Bureau of Mines Report No. 6862, 1966 (unpublished).

²¹J. R. Tessman, A. H. Kahn, and W. Shockley, Phys. Rev. **92**, 890 (1953).

²²S. Singh, D. A. Draegert, and J. E. Gusic, Phys. Rev. (to be published).

²³P. B. Jamieson, S. C. Abrahams, and J. L. Bernstein, J. Chem. Phys. **50**, 4352 (1969).

²⁴E. G. Spencer, P. V. Lenzo, and A. A. Ballman, Proc. IEEE **55**, 2074 (1967).

²⁵P. B. Jamieson, S. C. Abrahams, and J. L. Bernstein, J. Chem. Phys. **48**, 5048 (1968).

²⁶S. C. Abrahams and J. L. Bernstein, J. Phys. Chem. Solids **28**, 1685 (1967).

²⁷G. E. Peterson and P. M. Bridenbaugh, J. Chem. Phys. **46**, 4009 (1967); **48**, 3402 (1968).

²⁸J. A. Ditzenberger (unpublished).